Ultrasonic Guided Wave-Based Structural Health Monitoring for Early Detection and Localization of Multiple Damages in Composite Wind-Turbine Blades

AKSHAY PRAKASH KALGUTKAR, SHIRSENDU SIKDAR and SAUVIK BANERJEE

ABSTRACT

Wind energy plays a pivotal role in the transition to renewable energy sources. However, the reliability of wind turbine blades (WTBs) is often compromised by damage. This urges the increasing need for advanced Structural Health Monitoring (SHM) techniques to ensure the durability and reliability of WTBs. The current study investigates the application of the Ultrasonic Guided Wave (UGW) technique as a non-destructive evaluation (NDE) method for the early detection and localisation of multiple damages in composite WTBs. In this research, a network of three piezoelectric patches is strategically positioned on the blade's surface to excite guided waves and capture the scattered signals. The study focuses on localising the damages, such as impact damage, surface cracks and their combination. Finite Element (FE) modelling is utilised to simulate wave propagation in the complex composite WTB. A novel damage index mapping approach, based on signal energy difference and time-of-flight (ToF) analysis, is employed to approximate defect locations. The proposed methodology effectively demonstrates the capability to detect and locate the various damage types with significant accuracy. This research contributes to the advancement of intelligent SHM systems for wind energy applications, facilitating autonomous, data-driven maintenance strategies for efficient damage assessment.

KEYWORDS: Structural Health Monitoring, Ultrasonic Guided Waves, Composite Materials, Piezoelectric patches, Wind-Turbine Blades, Damage Localisation

INTRODUCTION

A key challenge for the future is developing cost-effective, non-polluting renewable energy sources to reduce dependence on conventional fuels. Wind turbine blades (WTBs), critical to wind energy systems, are typically made from composites for

Akshay Prakash Kalgutkar, Sauvik Banerjee, Department of Civil Engineering, Indian Institute of Technology Bombay, Powai, Mumbai-400076, India
Shirsendu Sikdar, School of Computing and Engineering, University of Huddersfield, Queensgate, Huddersfield- HD1 3DH, United Kingdom

their high strength-to-weight ratio [1]. Operating in harsh environments makes WTBs prone to damage, which can reduce efficiency and lead to failure. Early detection and accurate localisation of such damage are vital for reliable operation and optimized maintenance. Among various Structural Health Monitoring (SHM) techniques, ultrasonic guided waves (UGW) stand out for WTB inspection due to their long-range propagation, high sensitivity, and suitability for real-time monitoring. However, complex WTB geometries, varying thickness, and wave behaviours such as dispersion and mode conversion complicate real-time UGW-based inspection [2, 3].

Numerous studies have explored UGW techniques for WTB assessment. Tiwari, Raisutis [4] experimentally investigated using low-frequency UGWs to detect milled defects via energy and amplitude analysis. While Shoja, Berbyuk [5] conducted a numerical study with a specific focus on ice detection in WTBs. In contrast, Wang, Zhou [6] performed an experimental investigation using an array of piezoelectric (PZT) patches. Gómez Muñoz, García Marquez [7] experimentally inspected the delamination and layer separation in WTB based on correlations-based pattern recognition. Oliveira, Simas Filho [8] proposed bubble pulse-echo ultrasonic technology to acquire data, utilising wavelet denoising and principal component analysis for signal processing and extracting relevant defect features. Recently, the failure in the WTB was monitored by Chai, Wu [9] applied a multi-index UGW approach with Orthogonal Matching Pursuit (OMP) to improve defect localisation through a refined Probability-weighted Distribution Imaging (PDI) algorithm, resulting in an OMP-PDI localisation approach.

Research Gap and Scope of the Present Study

A review of the existing literature reveals that extensive research has been conducted on wave propagation and damage detection in WTBs affected by icing, and delamination. Additionally, limited attention has been given in detecting and locating damage, largely due to the complexities associated with varying thickness and curved sections in WTBs.

The current research aims to address these gaps by using UGW for accurate damage positioning. To achieve this objective, dispersion characteristics are analysed using a semi-analytical finite element (SAFE) approach. Additionally, a three-dimensional time-domain COMSOL Multiphysics® model couples solid mechanics and electrostatics to simulate surface cracks, impact dents, and their combination. To reduce sensor count, a novel weighted function-based damage mapping algorithm is proposed. This algorithm estimates the damage index (DI) using the time of flight (ToF) of the signal, incorporating a weighted function based on the sensing point distance to mitigate spurious DI peaks. The proposed approach promises to advance SHM of thin-walled WTBs, offering more precise, sensor-efficient damage detection for practical maintenance strategies.

FINITE ELEMENT MODELLING IN THE COMSOL MULTIPHYSICS

The present study focuses on locating the position of various damages in a glass fibre-reinforced polymer (GFRP) wind turbine blade (WTB) using circular piezoelectric (PZT) patches mounted on the blade surface. Finite element modelling is conducted using COMSOL Multiphysics® version 5.5 to simulate the response of a composite

turbine blade. To manage the complexity of the blade's geometry and significant curvature at the rear, the analysis focuses solely on the front segment of the blade of length 325 mm, as illustrated in Fig. 1. Due to the non-uniform thickness of the blade, its geometry is constructed in SolidWorks 2019 by dividing it into three distinct cross-sectional profiles, shown in Fig. 2. These profiles are joined using the loft feature to create the full 3D model of the blade.

In Fig. 2, '*X*' is the cross-section plane's longitudinal distance from the blade tip, '*W*' is the transverse distance of the point on a particular plane, '*h*' is the thickness of the consideration point and '*d*' is the depth of the point simulating the curvature from the edge surface. Three 10 mm diameter, 0.4 mm thick circular PZT patches bonded with a 0.1 mm epoxy layer to accommodate the curvature and ensure secure bonding, are strategically placed along the blade surface at regular intervals marked by 'd_s'. The primary objective of the study is to identify and localise multiple surface defects, specifically impact damage and cracks, on the wind turbine blade. These defects are numerically simulated by removing a specified depth of material from targeted surface areas within the designated region of interest as shown in Fig. 3.

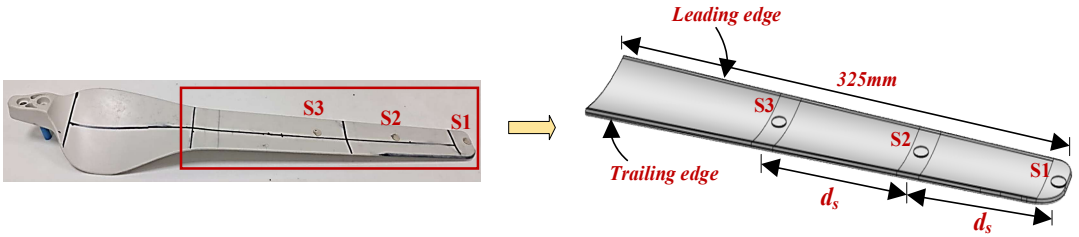

Figure 1. Idealisation of the mathematical model with respect to the experiment specimen.

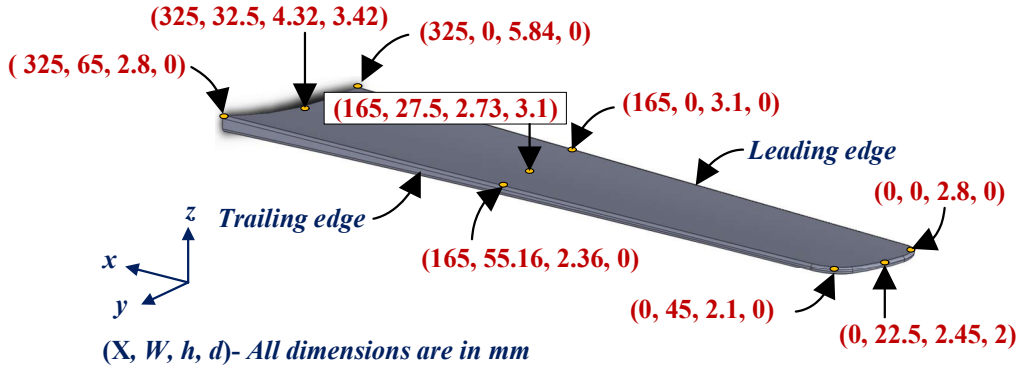

Figure 2. Mathematical model of wind turbine blade portion.

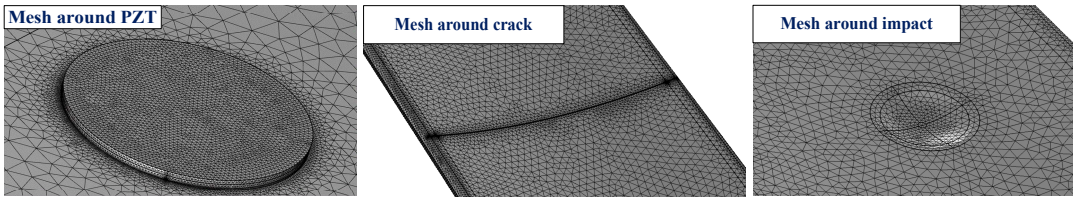

(a) (b) (c)

Figure 3. Meshing scheme around the (a) PZT, (b) crack and (c) impact damage

The present numerical modelling adopts a multiphysics approach, integrating the *Solid Mechanics* and *Electrostatics* modules via the *Piezoelectric Effect* interface to capture the coupled electromechanical behaviour. To accurately represent the fibre orientation along the blade's curved geometry, a curvilinear coordinate system is implemented, ensuring alignment of the local fibre axes with the blade's varying profile. A time-dependent study is conducted to simulate the dynamic behaviour of guided wave propagation within the wind turbine blade. The simulation procedure is systematically outlined in the flowchart presented in Fig. 4.

MATERIAL PROPERTIES

The material properties of woven carbon fibres considered for the composite laminated turbine blade are presented in Table 1. Table 2 describes the properties of the epoxy used for bonding the PZT patches to the turbine blade. Further, the material properties of the piezoelectric sensors PZT-5A employed in the simulation have been referred from the work of Qiu, Venkat [10] and have not been described here to avoid brevity.

Table 1. Material properties of carbon fibre reinforced woven composite.

E_{11} (GPa)	E_{22} (GPa)	E_{33} (GPa)	G_{12} (GPa)	G_{13} (GPa)	G_{23} (GPa)	ν_{12}	$\nu_{13}= \nu_{23}$	ρ (kg/m^3)
51.4	51.4	11.7	4.42	3.90	3.90	0.09	0.10	1630

Table 2. Material properties of epoxy used.

E (GPa)	G (GPa)	ν_{12}	ρ (kg/m^3)
4.94	1.803	0.37	1300

DAMAGE MAPPING METHOD

This section presents the methodologies employed for assessing damaged structures with available baseline (healthy state) data. A network of PZT sensors is utilised to define the inspection region encompassing potential damage sites. Damage localisation is further achieved by analysing variations between the baseline signals recorded in the pristine state and the signals obtained after damage has occurred.
In this work, the turbine blade is discretised into uniform grids of regularly spaced pixels. Damage images are generated by computing contrast values at each pixel derived from the damage index (DI) values estimated at different locations using the time of flight (ToF) from signals acquired through various pitch-catch transducer pairs. The fundamental Lamb modes A0 and S0 are used for constructing the damage mapping images based on energy difference-based signal features.

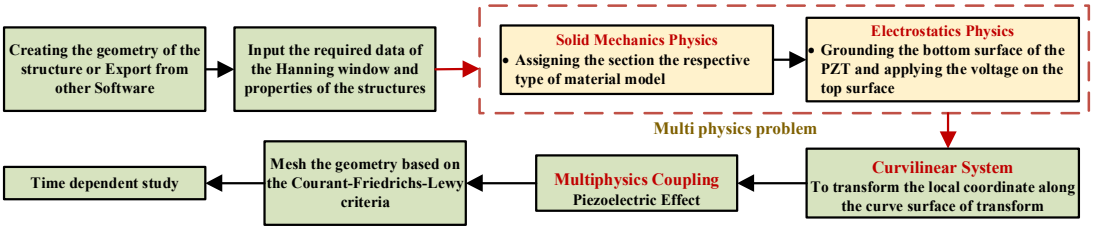

Figure 4. Flowchart of the simulation conducted in COMSOL Multiphysics® for GW propagation.

Given a total of '*N*' sensing paths within the sensor network, the probability of damage occurring at a specific grid point (*x, y*) can be determined as follows

$$P(x,y)=\sum_{i=1}^{N} DI_i(x,y)\cdot W(x,y) \tag{1}$$

Here, *W*(*x,y*) represents the weighted function that depends on the distance of the measurement point from the midpoint of the line connecting the actuator and receiver. For the k^{th} node in the discretised domain, *W(x,y)* is expressed as follows:

$$W(x,y)=\frac{d_{s-m}^2-d_{s-m,max}^2}{d_{s-m,min}^2-d_{s-m,max}^2};\quad d_{s-m}=\sqrt{(x-x_m)^2+(y-y_m)^2} \tag{2}$$

where $d_{s-m,max}$ and $d_{s-m,min}$ is the maximum and minimum value of the $d_{s\text{-}m}$ within the given structure grid. The weighted function exhibits a quadratic variation across the grid points, attaining a value of '1' at $d_{s-m,min}$ and '0' at $d_{s-m,max}$. This will aid in mitigating the abrupt rise in DI, thereby reducing the likelihood of false damage indications. DI_i is the energy difference-based damage index corresponding to the i^{th} sensing path is expressed by

$$DI_i(x,y)=\sum_{t=t_1}^{t_2}\left|S_d^i(t)^2-S_p^i(t)^2\right|_{S0}+\sum_{t=t_3}^{t_4}\left|S_d^i(t)^2-S_p^i(t)^2\right|_{A0} \tag{3}$$

where $S_d^i(t)$ and $S_p^i(t)$ are the amplitudes of the waveform for the i^{th} sensing path in the damaged and pristine states, respectively. The time range associated with the S0 mode are within 't_1' to 't_2', while 't_3' to 't_4' is the time range related to the A0 mode, as defined by

$$t_1=\frac{d_{s-a}+d_{s-r}}{C_g(x,y)\big|_{S0}};\quad t_2=t_1+\frac{n}{f};\quad t_3=\frac{d_{s-a}+d_{s-r}}{C_g(x,y)\big|_{A0}};\quad t_4=t_3+\frac{n}{f} \tag{4}$$

Here, C_g(*x,y*) is the group velocity of the wave mode at point (*x, y*). Additionally, (x_a, y_a) and (x_r, y_r) are the coordinates of the actuator and receiver PZTs on the i^{th} actuator-receiver pair, respectively, while (*x, y*) are the coordinates of the S point. The parameter $d_{s\text{-}a}$ refers to the distance between the actuator and the interested point 'S', whereas $d_{r\text{-}s}$ is the distance from point 'S' to the receiver, as noticed in Fig. 5.

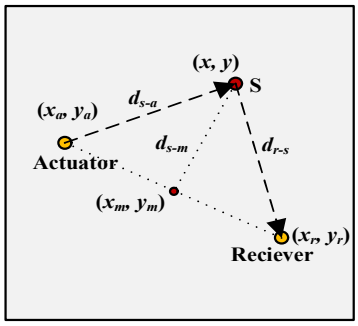

Figure 5. Imaging trajectory and illustration of relative distance.

After performing the DI mapping using Eq. (5) while incorporating the proposed weighted function, the final DI map [$WP(x,y)$] is generated. A threshold level (TL) is applied to approximate the location of the discontinuity in the structure, and is defined as follows.

$$WP(x,y) = \begin{cases} P(x,y), & if\ P(x,y) \geq TL \times max[P(x,y)] \\ 0 & Otherwise \end{cases} \tag{5}$$

The threshold level, ranging from 0.5 to 1, should be adjusted based on the magnitude of the peak DI value.

DISPERSION ANALYSIS

This section presents the analysis of group velocity dispersion and slowness curves for the composite plate. Despite the varying thickness of the turbine blade, it is essential to generate a dispersion curve by idealising the blade as a plate structure. Dispersion characteristics are obtained using the Semi-Analytical Finite Element (SAFE) method [11] to identify an optimal excitation frequency with minimal wave mode dispersion.

The dispersion curve, plotted along a 0° steering angle up to a frequency thickness product (f-h) value of 1.5 MHz-mm as shown in Fig. 6(a), indicates that the S0 mode maintains a nearly constant group velocity up to 750 kHz-mm before dropping sharply, indicating high dispersion at higher frequencies. In contrast, the A0 mode shows high dispersion below 450 kHz-mm with a rapid rise in velocity, which stabilises at higher frequencies. Given the blade's thickness range of 2.1 mm to 5.84 mm, the frequency–thickness product at 125 kHz excitation ranges from 260 to 730 kHz-mm. This lies within the non-dispersive range for both S0 and A0 modes, ensuring clear, well-separated wave packets. The corresponding slowness curves at 260 and 730 kHz-mm presented in Fig. 6(b) also show minimal directional dependence, resembling isotropic behaviour. Therefore, based on these observations, a 5-cycle Hanning window signal at a central frequency of 125 kHz will be employed to excite the actuator PZT in subsequent investigations.

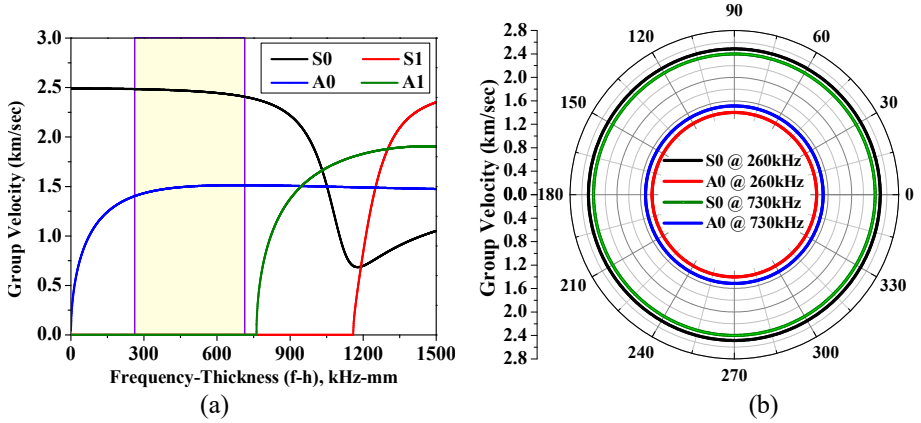

Figure 6. Dispersion curve of the thin composite plate along 0o steering angle, (b) Slowness curve of the composite plate excited at a frequency of 260 kHz and 730 kHz.

DAMAGE IMAGING AND LOCALISATION

This section details the use of a weighted function-based Damage Index (DI) mapping algorithm to localise impact and crack damage in a wind turbine blade, as discussed in Section 4. A 10 mm circular groove simulates impact damage, while a 0.2 mm deep line groove represents a surface crack. Numerical simulations in COMSOL Multiphysics® are performed with three PZTs placed 100 mm apart. Each PZT is excited sequentially, with the remaining two acting as sensors, resulting in six wave propagation paths.

Signals are recorded for both pristine and damaged states. The analysis focuses on energy differences at the time of arrival (TOA) of wave packets, considering both S0 and A0 modes. The group velocities are found to be 2.47 km/s (S0) and 1.48 km/s (A0). TOA values are computed based on actuator-receiver distances and wave velocities, and are used to calculate the weighted function and DI at various points.

A probability map of damage, P(x,y), is generated, and a 96% threshold of its peak value is applied to create the final DI map. Fig. 7 and Fig. 8 illustrate the effectiveness of the method for detecting cracks, impact damage, and their combination. Comparisons with simulated models confirm accurate damage localisation. Thus, the algorithm proves to be a simple yet effective tool for identifying surface cracks and impact dents in wind turbine blades.

CONCLUSION

The study focuses on detecting surface cracks and impact damage using a novel weighted function-based Damage Index (DI) mapping algorithm with ultrasonic guided waves (UGW). The method accurately localises damage using only three PZT

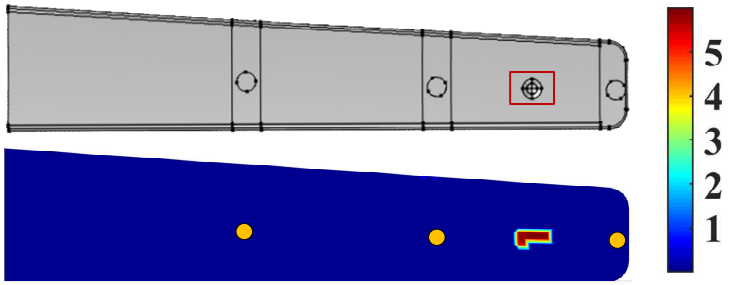

Figure 7. Numerical imaging outcome of the proposed weighted function-based damage mapping method in the WTB with an impact damage at an eccentricity of 50mm from the edge.

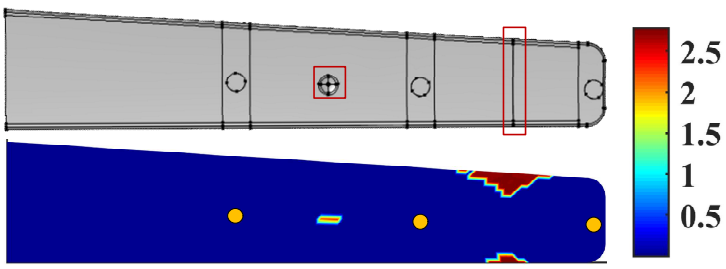

Figure 8. Imaging of the proposed weighted function-based damage mapping in the WTB with an impact damage at 150mm eccentricity and a surface crack at 50mm eccentricity from the edge.

patches, avoiding complex signal processing. A multiphysics finite element model is developed in COMSOL Multiphysics®, with a 125 kHz excitation frequency selected for its low dispersion, as noticed by SAFE-based dispersion and slowness curves.

The approach enhances NDE and SHM practices by enabling precise and efficient multi-damage localisation. It offers a scalable and efficient solution for guided wave-based multi-damage localisation, supporting more reliable and sustainable maintenance of wind turbine blades.

ACKNOWLEDGEMENTS

The authors gratefully acknowledge the Centre for Computational Engineering and Science (CCES) at IIT Bombay for providing the computing facilities.

REFERENCES

1. Cawley, P. and R.D. Adams, 1989."Defect types and non-destructive testing techniques for composites and bonded joints". *Materials Science and Technology*, 5(5): 413-425.
2. Guo, J., et al., 2017."Anisotropy in carbon fiber reinforced polymer (CFRP) and its effect on induction thermography". *NDT & E International*, 91: 1-8.
3. Prakash Kalgutkar, A. and S. Banerjee, 2024."Interaction of ultrasonic guided waves with interfacial debonding in a stiffened composite plate under variable temperature and operational conditions". *Ultrasonics*, 142: 107378.
4. Tiwari, K.A., R. Raisutis, and V. Samaitis, 2017."Hybrid Signal Processing Technique to Improve the Defect Estimation in Ultrasonic Non-Destructive Testing of Composite Structures". *Sensors*, 17(12).
5. Shoja, S., V. Berbyuk, and A. Boström, 2018."Guided wave–based approach for ice detection on wind turbine blades". *Wind Engineering*, 42(5): 483-495.
6. Wang, P., et al., 2018."Ice monitoring of a full-scale wind turbine blade using ultrasonic guided waves under varying temperature conditions". *Structural Control and Health Monitoring*, 25(4): e2138.
7. Gómez Muñoz, C.Q., et al., 2019."Structural health monitoring for delamination detection and location in wind turbine blades employing guided waves". *Wind Energy*, 22(5): 698-711.
8. Oliveira, M.A., et al., 2020."Ultrasound-based identification of damage in wind turbine blades using novelty detection". *Ultrasonics*, 108: 106166.
9. Chai, Y., et al., 2025."Failure monitoring and localization of wind turbine blades using ultrasonic guided waves and multi-index fusion imaging". *Engineering Failure Analysis*, 170: 109326.
10. Qiu, L., et al. *Multiphysics Simulation of Guided Wave Propagation under Load Condition*. in *8th International Symposium on NDT in Aerospace*. 2016. Bangalore, India: e-Journal of Nondestructive Testing.
11. Kalgutkar, A.P. and S. Banerjee, 2022."Semi-Analytical Finite Element Method for the Analysis of Guided Wave Dispersion in the Pre-stressed Composite Plates". *ASPS Conference Proceedings*, 1(5): 1413-1421.